Copyright © 2000 American Institute of Physics. This article may be downloaded for personal use only. Any other use requires prior permission of the author and the American Institute of Physics. This is a less abridged version of the letter we published on this topic in the 23 October, 2000 edition of Applied Physics Letters (Volume 77, Number 17, pp. 2698-2700), which may be found at
http://ojps.aip.org/journal_cgi/getabs?KEY=APPLAB&cvips=APPLAB000077000017002698000001

Size-dependent electrical behavior of spatially inhomogeneous barrier height regions on silicon

Robert C. Rossi[a)], Ming X. Tan[b)], and Nathan S. Lewis[c)]

Division of Chemistry and Chemical Engineering, 127-72, California Institute of Technology, Pasadena, California 91125

A series of ordered, periodic arrays of low barrier height n-Si/Ni nanometer-scale contacts interspersed among high barrier height n-Si/liquid contacts has been prepared, and the electrical properties of these heterostructures have been investigated as a function of scale. The arrays were formed by evaporating Ni through bilayers of close-packed latex spheres deposited on n-Si. By varying the diameter of the spheres from 174 nm to 1530 nm, geometrically self-similar Si/Ni structures were produced having triangular Si/Ni features ranging from approximately 100 to 800 nm on a side. The resulting Si surfaces were used as electrodes in methanolic electrochemical cells containing $LiClO_4$ and 1,1'-dimethylferrocene$^{+/o}$. The current-voltage and photoresponse properties of the resulting mixed barrier height contacts were strongly dependent on the size of the low barrier height contact regions even though the fraction of the Si surface covered by Ni remained constant. Electrodes formed from large-dimension Si/Ni and Si/liquid contacts behaved as expected for two (area-weighted) Schottky diodes operating independently and in parallel, whereas parallel nanoscale Si/Ni and Si/liquid contacts behaved in accord with effective barrier height theories predicting a "pinch-off" effect for mixed barrier height systems of sufficiently small physical dimensions.

[a)]Current address: Carleton College, Dept. of Chemistry, One North College St., Northfield, MN 55057; rrossi@carleton.edu

[b)]Current address: Sandia National Laboratory, P.O. Box 969, Livermore, CA 94551-9401

[c)]Author to whom correspondence should be addressed. Electronic mail: nslewis@its.caltech.edu

PACS numbers: 73.40.Ns, 73.40.Mr, 84.60.Dn, 85.40.Ux, 85.30.Hi, 85.30.De.

The electrical behavior of semiconductor/metal contacts having spatially inhomogeneous barrier heights has attracted much theoretical,[1,2] computational,[3-6] and experimental[7-13] attention.[14] Analytical theories[1,2] and numerical simulations[3-5] indicate that the current density through small, low barrier height regions on the surface of an otherwise high barrier height semiconductor/metal contact should be a strong function of the spatial dimensions of the low barrier height regions. Specifically, provided that the dimensions of the low barrier height regions are sufficiently small, and the band bending in the surrounding high barrier height regions is sufficiently large, the "effective" barrier height of such spatially inhomogeneous contacts is predicted to be much higher than that observed when the low barrier height regions act independently of the high barrier height regions (i.e., in a purely area-weighted fashion). Tung[1] coined the term "pinch-off" to describe this effect and argued that it might explain several widely-observed anomalies seen at semiconductor/metal contacts, including the T_o effect,[15] the observation of diode quality (ideality) factors greater than unity[1,2], and the discrepancies typically observed between Schottky barrier heights measured by differential capacitance-voltage (C-V) and current-voltage (I-V) techniques.[11,16] The pinch-off effect could also be important for semiconductor electrodes coated with nanoscopic metal islands, in that such electrodes could effectively direct minority carriers toward catalytic metal sites without incurring the majority carrier recombination effects[17,18] that would otherwise deleteriously affect the properties of a semiconductor interface having a high fraction of its area covered with low barrier height metal contacts. To our knowledge, however, the pinch-off phenomenon has not been unambiguously verified by experiment. Although semiconductor electrodes covered with discrete regions of differing barrier height may well display the pinch-off effect,[7,18-20] comparison between theory and experiment is difficult without reliable, independent knowledge of the area and barrier height of each region. Furthermore, recent numerical work questions the validity of the theories and simulations predicting the existence of the pinch-off phenomenon.[6]

For typical barrier height differences (0.3 V) and semiconductor dopant densities (1×10^{15} cm^{-3}) (and hence depletion widths of ca. 900 nm), the pinch-off phenomenon is expected to occur when the low barrier height regions are 400 nm or less in critical dimension λ and are surrounded by high barrier height regions extending for at least 2λ.[3] Because typical macroscopic electrical devices can not take advantage of a pinch-off effect that might arise from a single microscopic low barrier height region, observation of this putative effect in a macroscopic device requires methods to prepare large numbers of low barrier height regions, having well-defined contact areas and interfacial properties, surrounded by high barrier height contact regions. Our approach was to form ordered, periodic arrays of low barrier height Ni contacts on an etched (100)-oriented Si

surface. This was followed by the formation of a Si/liquid contact, which provided high barrier height regions on the unmetallized portions of the surface and a massively parallel electrical contact to the Ni features. n-Si/Ni diodes are poor rectifiers, having room-temperature exchange current densities J_o on the order of 10^{-4} A·cm^{-2}; these exchange currents are dominated by thermionic emission over a 0.62 V barrier height. In contrast, a solution of 1,1'-dimethylferrocene/1,1'-dimethylferrocenium ($Me_2Fc^{+/o}$) in methanol (CH_3OH) forms a high (≈ 1.0 V)[21] barrier height contact at n-Si, with recombination in forward bias dominated by minority carrier-based bulk recombination/diffusion processes at the Shockley diode limit.[17,21] Consequently, in the absence of interaction between the two different barrier height regions, a Ni contact covering as little as 1% of the surface[11] should significantly affect the I-V behavior of an n-Si electrode in contact with CH_3OH–$Me_2Fc^{+/o}$.

Our arrays were fabricated using nanosphere (or "natural") lithographic masks[22,23] prepared from commercially supplied polystyrene microspheres selected for the monodispersity of their sphere diameters. The substrates were all (100)-oriented, 5.6 ± 0.3 Ω·cm, P-doped, n-Si samples that were degreased, etched in buffered 49 wt% $HF_{(aq)}$ for 30 seconds, etched in concentrated $KOH_{(aq)}$ at ~38 °C for 4 min, and rinsed with 18 MΩ·cm resistivity H_2O. Crystalline structures of latex spheres, close-packed in the plane parallel to the substrate surface and two sphere layers thick, were produced using a procedure loosely analogous to Czochralski crystal growth, as detailed in Fig. 1(a).[24]

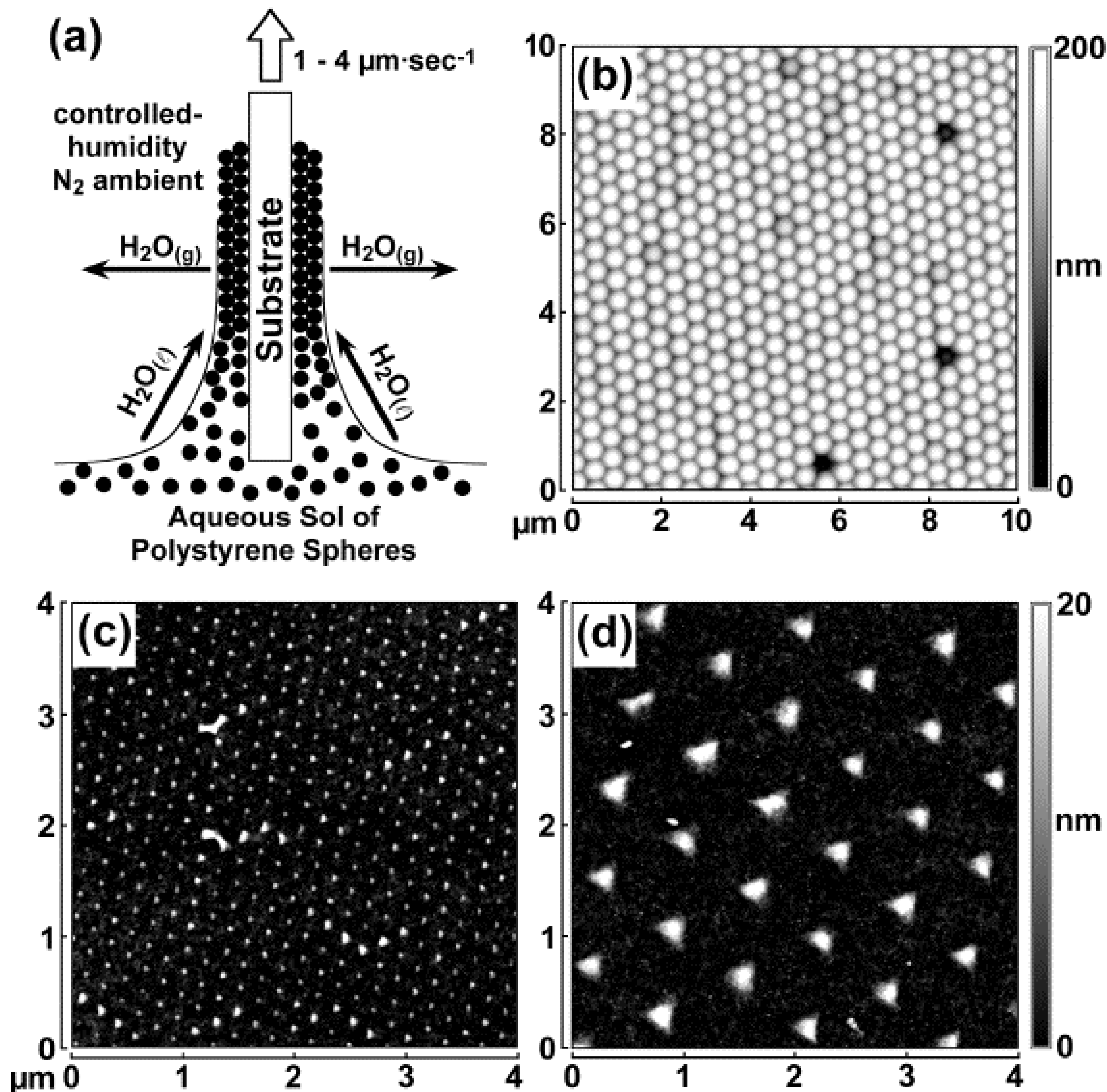

FIG. 1. Nanosphere lithography. (a) Hydrophillic Si was pulled vertically from aqueous sols of 2 - 10 $\%_{wt}$ monodispersed-diameter polystyrene spheres at 1 - 4 μm·s^{-1} under a controlled-humidity nitrogen ambient. Control of the sol concentration, pull speed, and ambient humidity, indexed to the diameter of the spheres used, allowed large areas (many mm^2) of two-layer close-packed sphere crystals to be grown. (b) Tapping-mode atomic force microscopy (TMAFM) image of a bilayer nanosphere lithographic mask consisting of 460 nm diameter polystyrene spheres grown on n-Si. The spheres in the lower layer (not visible) pack such that every other hole between the spheres in the top layer is blocked by a sphere in the layer beneath. The remaining holes have a clear view down to the substrate, and these define the Ni patterns left on the wafer after metal evaporation. Defective (undersized) spheres fill two of the point defects seen here, while the third point defect (at bottom edge of image) is completely empty in the top sphere layer. Importantly, defects in the top crystalline layer do not appear to correlate with defects in the layer below. Images (c) and (d) are of typical Ni dot patterns produced by deposition through a two-layer crystal mask composed of 174 nm and 760 nm diameter latex spheres, respectively. Point defects and dislocations present in the mask crystal are responsible for the defects in the nanopattern. Comparison of these two images (shown at the same scale) confirms that different sphere diameters produce metal dot arrays composed of dots of different sizes but arranged in self-similar patterns such that the fraction of the surface covered by Ni remains constant. Imaging conditions: Digital Instruments Nanoscope III employing TESP probes and a D (b) or E [(c) and (d)] scanner. Scan rate:1 Hz; Setpoint: 2.0 V (b), 0.736 V (c), 0.304 V (d); Free oscillation amplitude: 3.0 V (b), 1.0 V (c), 0.5 V (d); Scan size:12 μm (b), 4 μm (c), 4 μm (d); Integral gain: 0.591 (b), 0.512 [(c) and (d)]; Proportional gain: 5.45 (b), 5.86 [(c) and (d)].

Samples having overlayers prepared using a given sphere diameter [Fig. 1(b)] were divided into three groups. The members of the first group were sonicated in water to remove the spheres, and a macroscopic region masked off on each. They were not re-etched. All three sample groups were then transferred to a thermal evaporation system, where a thin (15 to 50 nm) layer of 99.994 wt% Ni was evaporated onto the first and second groups under an ambient pressure of $< 1 \times 10^{-6}$ Torr.[25] The third group was not exposed to the evaporated Ni. Sonication in water was then used to remove the spheres from the samples in the last two groups, and sonication in CH_3OH removed the mask material from the samples of the first group. None of the samples were re-etched at this point in the process. The ensemble thus consisted of one subset of Si samples covered with a continuous Ni layer (group 1), another subset covered with triangular Ni regions covering ≈ 8% of an otherwise bare surface[26] [group 2; Fig. 1(c) and 1(d)], and a third subset having completely bare surfaces (group 3). Electrodes were formed from these samples, and electrochemical experiments in contact with CH_3OH–1.0 M $LiClO_4$–100 mM Me_2Fc–15 mM $Me_2Fc^+BF_4^-$ solutions performed as described previously.[17] All samples were etched for 30 seconds in buffered 49 wt% $HF_{(aq)}$ immediately prior to their immersion in the electrolyte solution.

Dark current density-voltage (J-V) data were collected for many electrodes and corrected for cell resistance and concentration overpotential losses in the electrolyte. The data for a given type of electrode were then averaged to obtain a geometric mean current density at each of a variety of applied potentials. Figure 2 depicts the forward-bias J-V behavior of unmetallized, completely metallized, and nanoscale Ni-patterned n-Si electrodes, the latter as a function of the sphere size used in the mask process. Fitting these data to the diode equation,

$$J = \frac{\text{current}}{\text{electrode area}} = A^{**}T^2 \exp\left(\frac{-e\Phi_{b,eff}}{kT}\right)\left[\exp\left(\frac{-eV_{app}}{AkT}\right) - 1\right] \tag{1}$$

where T is the temperature, V_{app} the applied potential, e the charge on an electron, and k the Boltzmann constant, allowed the extraction of the effective barrier heights $\Phi_{b,eff}$ and diode quality factors A tabulated in Table I. The effective Richardson constant A^{**} used was 120 $A \cdot cm^{-2} \cdot T^{-2}$.

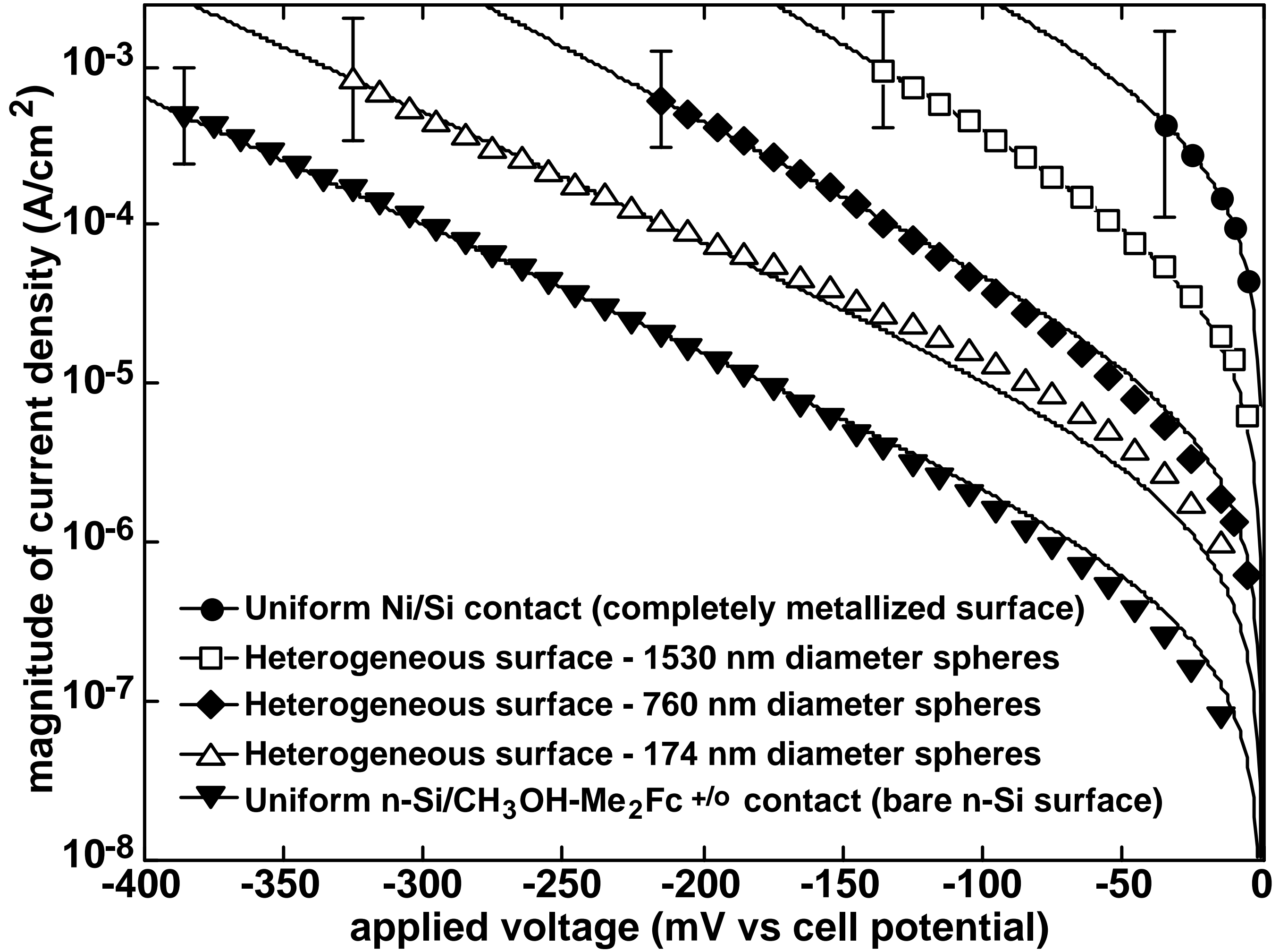

FIG. 2. Current-voltage properties of n-Si surfaces covered with Ni as indicated and immersed in CH_3OH–1.0 M $LiClO_4$–100 mM Me_2Fc–15 mM Me_2Fc^+ electrolyte. The data points shown are geometric mean currents calculated from the *n* electrodes of each type as indicated in Table I. The error bars shown are representative of the standard deviation in current seen along the entire length of a given curve. The smooth curves are the Levenberg-Marquardt fits to the diode equation [(Eq. 1)] used to extract the parameters listed in Table I.

TABLE I. Measured parameters for n-Si electrodes patterned with Ni and immersed in CH_3OH–1.0 M $LiClO_4$–100 mM Me_2Fc–15 mM $Me_2Fc^+BF_4^-$ solutions.

	Nature of electrode surface				
	Bare Si	Nanopatterned	Nanopatterned	Nanopatterned	Ni/Si
Sphere diameter used in mask[a] (nm)	n/a	174 ± 2	760 ± 1.4	1530 ± 18	n/a
Effective Ni dot diameter[b,c] (nm)	n/a	55 ± 13	210 ± 50	510 ± 120	n/a
Interparticle spacing[d] (nm)	n/a	203 ± 5	763 ± 19	1630 ± 50	n/a
Fractional coverage of Ni[c]	0 %	7.1 ± 0.7 %	7.1 ± 1.0 %	9.0 ± 1.1 %	100 %
Exchange current density, J_o ($\mu A/cm^2$)	0.40	1.8	6.3	41	431
Effective barrier height,[e] $\Phi_{b,eff}$ (V)	0.80 ± 0.04	0.76 ± 0.05	0.72 ± 0.03	0.68 ± 0.02	0.62 ± 0.04
Diode quality (ideality) factor, A	2.1	2.1	1.8	1.7	1.9
Measurement Temperature, T (°C)	25.3 ± 1.7	25.7 ± 1.4	25.6 ± 0.8	26.5 ± 1.1	25.8 ± 1.1
Number of samples, n	25	14	8	7	25

[a]Manufacturers' reported physical diameters as obtained by transmission electron or optical microscopy
[b]Diameter of a circular dot having the same area as the triangular Ni dot formed
[c]Obtained by tapping-mode atomic force microscopy, these values are approximate–the uncertainty indicated reflects only the variability in measurements themselves
[d]Distance between centers of nearest-neighbor particles on patterned surface
[e]Barrier height that would give the measured exchange current density assuming thermionic emission to be the dominant recombination mechanism

Completely metallized n-Si/Ni contacts exhibited current transport properties indicative of a barrier height of 0.62 ± 0.04 V. In contrast, the n-Si/CH_3OH–$Me_2Fc^{+/o}$ contacts exhibited excellent rectification properties and relatively small currents under forward bias, consistent with prior measurements quantifying the relatively high barrier height and relatively low majority carrier interfacial capture velocity of this semiconductor/liquid contact.[17,21] The J-V behavior of the Si electrodes patterned with Ni was clearly intermediate between that of a homogeneous Si/Ni Schottky contact and that of a homogeneous Si/CH_3OH–$Me_2Fc^{+/o}$ contact. Furthermore, electrodes exhibited progressively better rectification properties as the size of the Ni features became smaller, even though the fraction of the electrode area covered by Ni was essentially constant for all the nanoscale-patterned surfaces due to the self-similarity provided by the nanosphere lithographic method.

The observations described above are in excellent agreement with the behavior predicted by the existence of the pinch-off effect. The current-transport properties of these Ni-patterned electrodes suggest that the effective barrier height experienced by majority carriers approaching the nanopatterned contacts is higher than the barrier height of a uniform Si/Ni contact. The observed currents for the nanopatterned electrodes are appreciably lower than those expected from an area-weighted summation of the currents expected through independent Si/Ni and Si/CH_3OH–$Me_2Fc^{+/o}$ contacts. Furthermore, for sufficiently small nanopatterned contacts, the J-V properties of the nanopatterned electrodes approached those of a bare Si surface, even though a significant fraction of the nanopatterned surface was covered with low barrier height Ni/Si contacts. The natural explanation of these observations is that the pinch-off phenomenon ensures that the low barrier height regions have little influence on the overall majority carrier transport processes through the nanopatterned Si/Ni surface.

The J-V behavior depicted in Fig. 2 is in good agreement with that predicted by Tung[2] and Sullivan et al.[3] for these mixed barrier height contacts, given the size of the Ni contacts, the dopant density of the Si, and the rectification properties of the homogenous Si/Ni and Si/liquid contacts studied in this work. To ascertain whether quantitative differences exist between theory and experiment, simulation of each individual electrode region and a concurrent analysis of the electrochemical behavior of each electrode will be required to account for the effects of variability in the size of the Si/Ni contacts, defects in the array, and variability in the J-V properties of the homogeneous contacts. However, it is clear that the general behavior predicted to result from the pinch-off phenomenon is observed in these nanopatterned electrodes. With regard to semiconductor/liquid contacts, we note that the pinch-off effect provides a means to introduce catalytically active metal sites on the semiconductor surface – thus promoting desirable minority carrier-based multi-electron transfer reactions –

without suffering deleterious majority-carrier-based recombination. Utilizing this principle we hope to produce desirable, novel behavior in photoelectrodes. Efforts are also underway to investigate the J-V behavior of mixed barrier height systems in purely solid-state contacts, and to compare J-V properties with C-V properties on both macro- and micro- scales.

The authors acknowledge the National Science Foundation, grant CHE-9974562, for support of this research, and R. R. thanks the NSF for a graduate fellowship.

References

[1] R. T. Tung, Appl. Phys. Lett. **58,** 2821-3 (1991).
[2] R. T. Tung, Phys. Rev. B **45,** 13509-23 (1992).
[3] J. P. Sullivan, R. T. Tung, M. R. Pinto, and W. R. Graham, J. Appl. Phys. **70,** 7403-24 (1991).
[4] J. L. Freeouf, T. N. Jackson, S. E. Laux, and J. M. Woodall, J. Vac. Sci. Technol. **21,** 570-3 (1982).
[5] I. Ohdomari and H. Aochi, Phys. Rev. B **35,** 682-6 (1987).
[6] J. Osvald, J. Appl. Phys. **85,** 1935-42 (1999).
[7] S. Anand, S. B. Carlsson, K. Deppert, L. Montelius, and L. Samuelson, J. Vac. Sci. Technol. B **14,** 2794-8 (1996).
[8] A. Olbrich, J. Vancea, F. Kreupl, and H. Hoffmann, J. Appl. Phys. **83,** 358-65 (1998).
[9] M. V. Schneider, A. Y. Cho, E. Kollberg, and H. Zirath, Appl. Phys. Lett. **43,** 558-60 (1983).
[10] P. Niedermann, L. Quattropani, K. Solt, A. D. Kent, and O. Fischer, J. Vac. Sci. Technol. B **10,** 580-5 (1992).
[11] I. Ohdomari, T. S. Kuan, and K. N. Tu, J. Appl. Phys. **50,** 7020-9 (1979).
[12] H. Palm, M. Arbes, and M. Schulz, Phys. Rev. Lett. **71,** 2224-7 (1993).
[13] A. A. Talin, R. S. Williams, B. A. Morgan, K. M. Ring, and K. L. Kavanagh, J. Vac. Sci. Technol. B **12,** 2634-8 (1994).
[14] R. T. Tung, J. P. Sullivan, and F. Schrey, Mat. Sci. Eng. B **14,** 266-80 (1992).
[15] M. S. Tyagi, in *Metal-Semiconductor Schottky Barrier Junctions and Their Applications*, edited by B. L. Sharma (Plenum, New York, 1984).
[16] E. H. Rhoderick and R. H. Williams, *Metal-Semiconductor Contacts*, 2nd ed. (Oxford University Press, New York, 1988).
[17] A. Kumar and N. S. Lewis, J. Phys. Chem. **95,** 7021-28 (1991).
[18] Y. Nakato, K. Ueda, H. Yano, and H. Tsubomura, J. Phys. Chem. **92,** 2316-24 (1988), and references therein.
[19] S. Yae, R. Tsuda, T. Kai, K. Kikuchi, M. Uetsuji, T. Fuji, M. Fujitani, and Y. Nakato, J. Electrochem. Soc. **141,** 3090-5 (1994).
[20] A. Meier, I. Uhlendorf, and D. Meissner, Electrochim. Acta **40,** 1523-35 (1995).
[21] P. E. Laibinis, C. E. Stanton, and N. S. Lewis, J. Phys. Chem. **98,** 8765-74 (1994).
[22] H. W. Deckman and J. H. Dunsmuir, Appl. Phys. Lett. **41,** 377-9 (1982).
[23] J. C. Hulteen and R. P. Van Duyne, J. Vac. Sci. Technol. A **13,** 1553-8 (1995).
[24] A. S. Dimitrov and K. Nagayama, Langmuir **12,** 1303-11 (1996).
[25] A 45 mm long uncollimated source was positioned 120 mm or 250 mm directly above the substrates.
[26] Quoted metal coverages are approximate, having been extracted from atomic force microscopy images uncorrected for tip convolution effects. See J. C. Hulteen, D. A. Treichel, M. T. Smith, M. L. Duval, T. R. Jensen, and R. P. Van Duyne, Journal of Physical Chemistry B **103,** 3854-63 (1999) for a discussion of such corrections. The edges of the metal particles were indistinct in our images, so our metal coverage measurements would remain approximate even if corrected for tip convolution. Idealized geometric considerations predict fractional surface coverages between 3% and 4% for double-layer nanosphere lithographic masks.